

First Measurement of $\Gamma(D^{*+})$

S. Ahmed,¹ M. S. Alam,¹ S. B. Athar,¹ L. Jian,¹ L. Ling,¹ M. Saleem,¹ S. Timm,¹ F. Wappler,¹ A. Anastassov,² E. Eckhart,² K. K. Gan,² C. Gwon,² T. Hart,² K. Honscheid,² D. Hufnagel,² H. Kagan,² R. Kass,² T. K. Pedlar,² J. B. Thayer,² E. von Toerne,² M. M. Zoeller,² S. J. Richichi,³ H. Severini,³ P. Skubic,³ A. Undrus,³ V. Savinov,⁴ S. Chen,⁵ J. W. Hinson,⁵ J. Lee,⁵ D. H. Miller,⁵ E. I. Shibata,⁵ I. P. J. Shipsey,⁵ V. Pavlunin,⁵ D. Cronin-Hennessy,⁶ A. L. Lyon,⁶ W. Park,⁶ E. H. Thorndike,⁶ T. E. Coan,⁷ Y. S. Gao,⁷ Y. Maravin,⁷ I. Narsky,⁷ R. Stroynowski,⁷ J. Ye,⁷ T. Wlodek,⁷ M. Artuso,⁸ K. Benslama,⁸ C. Boulahouache,⁸ K. Bukin,⁸ E. Dambasuren,⁸ G. Majumder,⁸ R. Mountain,⁸ T. Skwarnicki,⁸ S. Stone,⁸ J. C. Wang,⁸ A. Wolf,⁸ S. Kopp,⁹ M. Kostin,⁹ A. H. Mahmood,¹⁰ S. E. Csorna,¹¹ I. Danko,¹¹ V. Jain,^{11*} K. W. McLean,¹¹ Z. Xu,¹¹ R. Godang,¹² G. Bonvicini,¹³ D. Cinabro,¹³ M. Dubrovin,¹³ S. McGee,¹³ A. Bornheim,¹⁴ E. Lipeles,¹⁴ S. P. Pappas,¹⁴ A. Shapiro,¹⁴ W. M. Sun,¹⁴ A. J. Weinstein,¹⁴ D. E. Jaffe,¹⁵ R. Mahapatra,¹⁵ G. Masek,¹⁵ H. P. Paar,¹⁵ A. Eppich,¹⁶ T. S. Hill,¹⁶ R. J. Morrison,¹⁶ H. N. Nelson,¹⁶ R. A. Briere,¹⁷ G. P. Chen,¹⁷ T. Ferguson,¹⁷ H. Vogel,¹⁷ J. P. Alexander,¹⁸ C. Bebek,¹⁸ B. E. Berger,¹⁸ K. Berkelman,¹⁸ F. Blanc,¹⁸ V. Boisvert,¹⁸ D. G. Cassel,¹⁸ P. S. Drell,¹⁸ J. E. Duboscq,¹⁸ K. M. Ecklund,¹⁸ R. Ehrlich,¹⁸ P. Gaidarev,¹⁸ L. Gibbons,¹⁸ B. Gittelman,¹⁸ S. W. Gray,¹⁸ D. L. Hartill,¹⁸ B. K. Heltsley,¹⁸ L. Hsu,¹⁸ C. D. Jones,¹⁸ J. Kandaswamy,¹⁸ D. L. Kreinick,¹⁸ M. Lohner,¹⁸ A. Magerkurth,¹⁸ H. Mahlke-Krüger,¹⁸ T. O. Meyer,¹⁸ N. B. Mistry,¹⁸ E. Nordberg,¹⁸ M. Palmer,¹⁸ J. R. Patterson,¹⁸ D. Peterson,¹⁸ D. Riley,¹⁸ A. Romano,¹⁸ H. Schwarhoff,¹⁸ J. G. Thayer,¹⁸ D. Uner,¹⁸ B. Valant-Spaight,¹⁸ G. Viehhauser,¹⁸ A. Warburton,¹⁸ P. Avery,¹⁹ C. Prescott,¹⁹ A. I. Rubiera,¹⁹ H. Stoeck,¹⁹ J. Yelton,¹⁹ G. Brandenburg,²⁰ A. Ershov,²⁰ D. Y.-J. Kim,²⁰ R. Wilson,²⁰ B. I. Eisenstein,²¹ J. Ernst,²¹ G. E. Gladding,²¹ G. D. Gollin,²¹ R. M. Hans,²¹ E. Johnson,²¹ I. Karliner,²¹ M. A. Marsh,²¹ C. Plager,²¹ C. Sedlack,²¹ M. Selen,²¹ J. J. Thaler,²¹ J. Williams,²¹ K. W. Edwards,²² A. J. Sadoff,²³ R. Ammar,²⁴ A. Bean,²⁴ D. Besson,²⁴ X. Zhao,²⁴ S. Anderson,²⁵ V. V. Frolov,²⁵ Y. Kubota,²⁵ S. J. Lee,²⁵ R. Poling,²⁵ A. Smith,²⁵ C. J. Stepaniak,²⁵ and J. Urheim²⁵

(CLEO Collaboration)

¹State University of New York at Albany, Albany, New York 12222

²Ohio State University, Columbus, Ohio 43210

³University of Oklahoma, Norman, Oklahoma 73019

⁴University of Pittsburgh, Pittsburgh, Pennsylvania 15260

⁵Purdue University, West Lafayette, Indiana 47907

⁶University of Rochester, Rochester, New York 14627

⁷Southern Methodist University, Dallas, Texas 75275

⁸Syracuse University, Syracuse, New York 13244

⁹University of Texas, Austin, Texas 78712

¹⁰University of Texas–Pan American, Edinburg, Texas 78539

¹¹Vanderbilt University, Nashville, Tennessee 37235

¹²Virginia Polytechnic Institute and State University, Blacksburg, Virginia 24061

¹³Wayne State University, Detroit, Michigan 48202

¹⁴California Institute of Technology, Pasadena, California 91125

¹⁵University of California–San Diego, La Jolla, California 92093

¹⁶University of California, Santa Barbara, California 93106

¹⁷Carnegie Mellon University, Pittsburgh, Pennsylvania 15213

¹⁸Cornell University, Ithaca, New York 14853

¹⁹University of Florida, Gainesville, Florida 32611

²⁰Harvard University, Cambridge, Massachusetts 02138

²¹University of Illinois, Urbana-Champaign, Illinois 61801

²²Carleton University, Ottawa, Ontario, Canada K1S 5B6

and the Institute of Particle Physics, Canada

²³Ithaca College, Ithaca, New York 14850

²⁴University of Kansas, Lawrence, Kansas 66045

²⁵University of Minnesota, Minneapolis, Minnesota 55455

(Received 7 August 2001; published 28 November 2001)

We present the first measurement of the D^{*+} width using 9/fb of e^+e^- data collected near the $Y(4S)$ resonance by the CLEO II.V detector. Our method uses advanced tracking techniques and a reconstruction method that takes advantage of the small vertical size of the Cornell Electron-positron Storage Ring beam spot to measure the energy release distribution from the $D^{*+} \rightarrow D^0\pi^+$ decay. We

find $\Gamma(D^{*+}) = 96 \pm 4$ (stat) ± 22 (syst) keV. We also measure the energy release in the decay and compute $\Delta m \equiv m_{D^{*+}} - m_{D^0} = 145.412 \pm 0.002$ (stat) ± 0.012 (syst) MeV/c².

DOI: 10.1103/PhysRevLett.87.251801

PACS numbers: 13.25.Ft, 14.40.Lb

A measurement of $\Gamma(D^{*+})$ opens an important window on the nonperturbative strong physics involving heavy quarks. The basic framework of the theory is well understood; however, there is still much speculation—predictions for the width range from 15 to 150 keV [1]. We know the D^{*+} width is dominated by strong decays. The level splitting in the B sector is not large enough to allow real strong transitions. Therefore, a measurement of the width of the D^{*+} gives unique information about the strong coupling constant in heavy-light meson systems. This width depends only on g , a universal strong coupling between heavy vector and pseudoscalar mesons to the pion, since the small contribution of the electromagnetic decay can be neglected, yielding

$$\Gamma(D^{*+}) = \frac{2g^2}{12\pi f_\pi^2} p_{\pi^+}^3 + \frac{g^2}{12\pi f_\pi^2} p_{\pi^0}^3, \quad (1)$$

where f_π is the pion decay constant and the momenta are for the indicated particle in D^{*+} decay in the D^{*+} rest frame [2].

Prior to this measurement, the D^{*+} width was limited to be less than 131 keV at the 90% confidence level by the ACCMOR collaboration [3]. This Letter describes a measurement of the D^{*+} width with the CLEO II.V detector [4]. The signal is reconstructed through a single, well-measured sequence, $D^{*+} \rightarrow \pi_{\text{slow}}^+ D^0, D^0 \rightarrow K^- \pi^+$.

The CLEO detector has been described in detail elsewhere. All of the data used in this analysis are taken with the detector in its II.V configuration [5]. The data were taken in symmetric e^+e^- collisions at a center of mass energy around 10 GeV with an integrated luminosity of 9.0/fb provided by the Cornell Electron-positron Storage Ring (CESR). The nominal sample follows the selection of $D^{*+} \rightarrow \pi_{\text{slow}}^+ D^0 \rightarrow K^- \pi^+ \pi_{\text{slow}}^+$ candidates used in our $D^0 - \bar{D}^0$ mixing analysis [6].

Our reconstruction method takes advantage of the small CESR beam spot and the kinematics and topology of the $D^{*+} \rightarrow \pi_{\text{slow}}^+ D^0 \rightarrow \pi_{\text{slow}}^+ K^- \pi^+$ decay chain. The K^- and π^+ are required to form a common vertex. The resultant D^0 candidate momentum vector is then projected back to the CESR luminous region to determine the D^0 production point. The CESR luminous region has a Gaussian width $\sim 10 \mu\text{m}$ vertically and $\sim 300 \mu\text{m}$ horizontally. This procedure determines an accurate D^0 production point for D^0 's moving out of the horizontal plane. Then the π_{slow}^+ track is refit constraining its trajectory to intersect the D^0 production point. This improves the resolution on the energy release, $Q = M(K^- \pi^+ \pi_{\text{slow}}^+) - M(K^- \pi^+) - m_{\pi^+}$, by more than 30% over simply forming the appropriate invariant masses of the tracks. The distribution of our resolution, σ_Q , is shown in Fig. 1 and is typically 150 keV. The good

agreement between Monte Carlo and data demonstrates that the kinematics and sources of uncertainties on the tracks, such as the number of hits used and the effects of multiple scattering in detector material, are well modeled.

The challenge of measuring the width of the D^{*+} is understanding the tracking system response function since the experimental resolution exceeds the width we are trying to measure. We depend on exhaustive comparisons between a GEANT [7] based detector simulation and our data. We addressed the problem by selecting samples of candidate D^{*+} decays using three strategies.

First, we produced the largest sample from data and simulation by imposing only basic tracking consistency requirements. We call this the *nominal* sample. Second, we refine the nominal sample selecting candidates with the best measured tracks by making very tight cuts on tracking parameters. We call this the *tracking selected* sample. A third alternative is to select our data on specific kinematic properties of the D^{*+} decay that minimize the dependence of the width of the D^{*+} on detector mismeasurements. We call this the *kinematic selected* sample. In all three samples the width is extracted with an unbinned maximum likelihood fit to the energy release distribution. These three different approaches yield consistent values for the width of the D^{*+} giving us confidence that our simulation accurately models our data.

To further improve the quality of reconstruction in our sample, we apply some selections at the kinematic boundaries of π_{slow}^+ momentum and the opening angle θ between

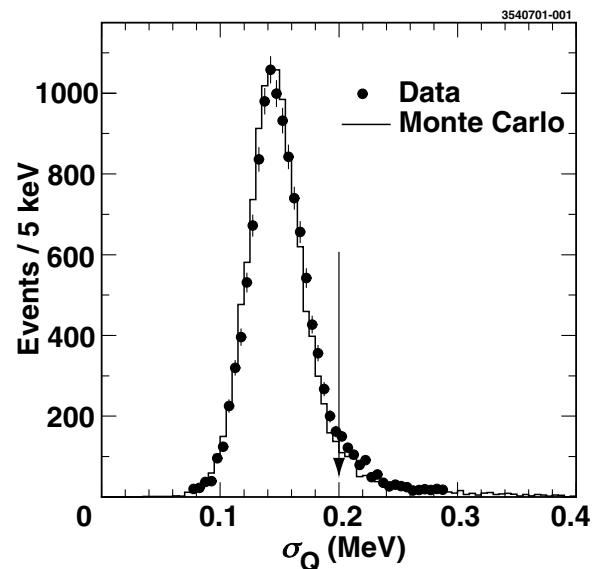


FIG. 1. Distribution of σ_Q ; the uncertainty on Q as determined from propagating track fitting errors. The arrow indicates our selection to remove the long tail in the error distribution.

TABLE I. The data sample, results of the fits, and simulation biases. The uncertainties are only statistical.

Parameter	Sample		
	Nominal	Tracking	Kinematic
Candidates	11 496	368	3284
N_{signal}	$11\,207 \pm 109$	353 ± 20	3151 ± 57
$N_{\text{background}}$	289 ± 31	15 ± 7	133 ± 16
f_{mis} (%)	5.3 ± 0.5	NA	NA
σ_{mis} (keV)	508 ± 39	NA	NA
Q_0 (keV)	5853 ± 2	5854 ± 10	5850 ± 4
Γ_0 (keV)	98.9 ± 4.0	106.0 ± 19.6	108.1 ± 5.9
$\Gamma_{\text{fit}} - \Gamma_{\text{generated}}$ (keV)	2.7 ± 2.1	1.7 ± 6.4	4.3 ± 3.1
D^{*+} width (keV)	96.2 ± 4.0	104 ± 20	103.8 ± 5.9

the π_{slow}^+ and the D^0 candidate as a function of the D^{*+} candidate momentum distributions to remove a small amount of misreconstructed signal and background. We also require $\sigma_Q < 200$ keV which removes the long tail in the error distribution.

Table I summarizes the statistics in our three samples. The tracking and kinematic samples are subsets of the nominal sample. The two subsets contain 94 common candidates.

We assume that the intrinsic width of the D^0 is negligible, $\Gamma(D^0) \ll \Gamma(D^{*+})$, implying that the width of Q is simply a convolution of the shape given by the D^{*+} width and the tracking system response function. Thus we consider the pairs of Q and σ_Q for $D^{*+} \rightarrow \pi_{\text{slow}}^+ D^0 \rightarrow K^- \pi^+ \pi_{\text{slow}}^+$, where σ_Q is given for each candidate by propagating the tracking errors in the kinematic fit of the charged tracks.

The underlying signal shape of the Q distribution is assumed to be given by a P -wave Breit-Wigner with central value Q_0 . We considered a relativistic and nonrelativistic Breit-Wigner as a model of the underlying signal shape, and found negligible changes in the fit parameters between the two. The width of the signal Breit-Wigner depends on Q and is given by

$$\Gamma(Q) = \Gamma_0 \left(\frac{P}{P_0} \right)^3 \left(\frac{M_0}{M} \right)^2, \quad (2)$$

where $\Gamma_0 \equiv \Gamma(D^{*+})$, P and M are the candidate π_{slow}^+ or D^0 momentum in the D^{*+} rest frame and $K\pi\pi_{\text{slow}}$ mass, and P_0 and M_0 are the values computed using Q_0 . The effect of the mass term is negligible at our energy. The partial width and the total width differ negligibly in their dependence on Q for $Q > 1$ MeV.

For each candidate the signal shape is convolved with a resolution Gaussian with width σ_Q , determined by the tracking errors, as a model of our resolution. The fit also includes a background contribution with a fixed shape derived from our simulation, and modeled with a third order polynomial. We allow a small fraction of the signal, f_{mis} , to be parametrized by a single Gaussian resolution function of width σ_{mis} . This shape is included in the fit to

model the tracking mishaps which our simulation predicts to be at the 5% level in the nominal sample and negligible in both the tracking and kinematic selected samples. In our standard fit we constrain the level of this contribution while allowing σ_{mis} to float.

As a preliminary test to fitting the data, we run the complete analysis on a fully simulated sample that has about 10 times the data statistics and is generated with a range of underlying $\Gamma(D^{*+})$ from 0 to 130 keV. We do this for the three samples and compute offsets between the generated and the fit values for the width and the mean energy release. The offset is consistent with zero as a function of the generated width of the D^{*+} . Table II summarizes this simulation study. We apply the weighted average of these offsets to the fit value that we obtain from the data. For the energy release, Q_0 , all samples show small shifts: -7 ± 3 keV for the nominal, -12 ± 10 keV for the tracking, and -12 ± 5 keV for the kinematic.

Figure 2 displays the fits to the three data samples. The results of the fits are summarized in Table I.

The agreement is excellent among the three fits, and when the offsets from Table I are applied we obtain the results given in the last row. The uncertainties are only statistical.

We discuss the sources of systematic uncertainties on our measurements of the width of the D^{*+} in the order of their size. The most important contribution is the variation of the results as a function of the kinematic parameters of the D^{*+} decay. The next most important contribution

TABLE II. Summary of fits to the simulated samples.

$\Gamma_{\text{generated}}$ (keV)	$\Gamma_{\text{fit}} - \Gamma_{\text{generated}}$ (keV) in sample		
	Nominal	Tracking	Kinematic
70	2.2 ± 5.0	-6.0 ± 12.4	11.7 ± 7.1
80	2.7 ± 5.2	-5.2 ± 14.2	3.9 ± 7.4
90	7.2 ± 5.7	33.5 ± 21.4	19.5 ± 8.8
100	-2.2 ± 5.4	4.1 ± 18.2	-6.3 ± 7.8
110	-2.7 ± 5.7	-9.2 ± 18.8	-5.4 ± 8.3
120	7.1 ± 6.1	18.2 ± 21.5	7.7 ± 9.3
130	6.9 ± 6.4	2.8 ± 18.7	-1.0 ± 9.4

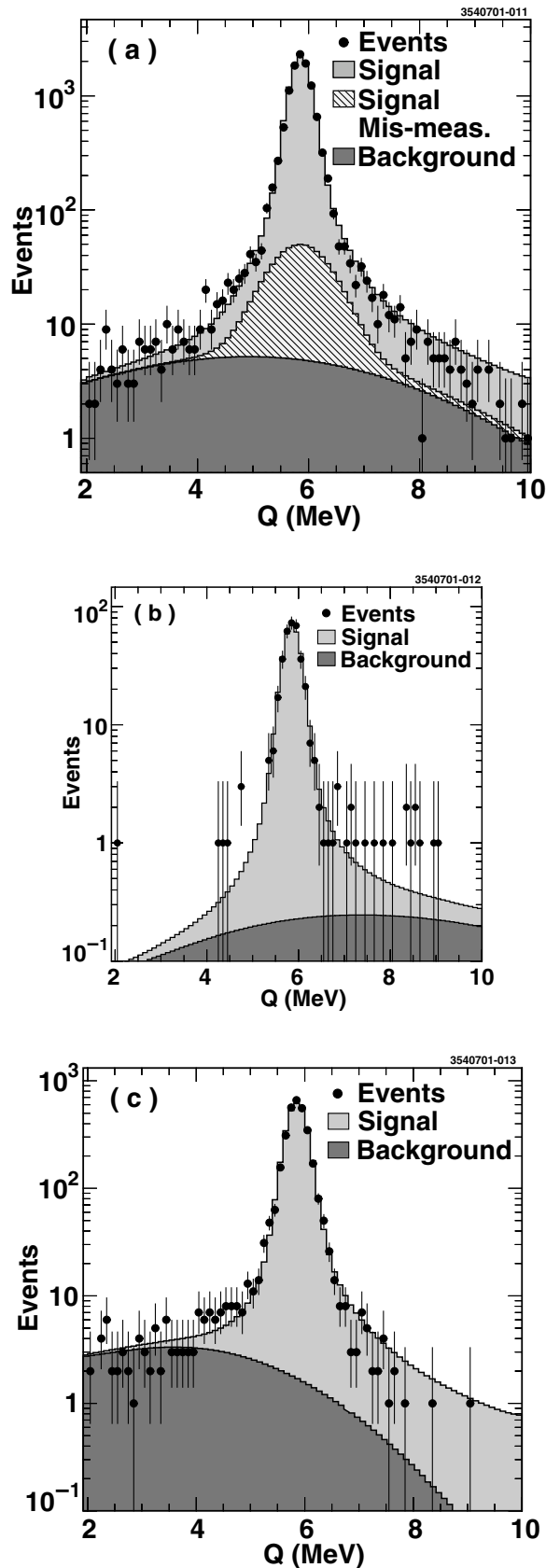


FIG. 2. Fits to the three data samples: (a) nominal; (b) tracking; and (c) kinematic. The different contributions to the fits are shown by different shades or patterns.

comes from any mismodeling of σ_Q dependence on the kinematic parameters. We take into account correlations among the less well measured parameters of the fit, such as f_{mis} and σ_{mis} , by fixing each parameter at $\pm 1\sigma$ from their central fit values, repeating the fit, and adding in quadrature the variation in the width of the D^{*+} and Q_0 from their central values. We have studied in the simulation the sources of mismeasurement that give rise to smearing on the width of the D^{*+} . The only source of smearing that we cannot account for is a small distortion of the kinematics of the event caused by the algorithm used to reconstruct the D^0 origin point described above. We have also checked that our simulation accurately models the line shape of other narrow resonances visible in our data. Notably, the decay $\Lambda^0 \rightarrow p\pi^-$, when we select the π^- to have a momentum in the range of the π_{slow}^+ in the D^{*+} decay, has a visible width which agrees to a few percent between data and simulation. We consider uncertainties from the background shape by allowing the coefficients of the background polynomial to float. Minor sources of uncertainty are from the width offsets derived from our simulation and given in Table I, and our digitized data storage format.

An extra and dominant source of uncertainty on Q_0 is the energy scale of our measurements. We evaluate this uncertainty by studying $K_s \rightarrow \pi^+\pi^-$ decays in our data. In order to bring the K_s mass central value in agreement with the nominal one, we make small relative momentum corrections, less than 0.3%, for tracks with momenta between 100 and 500 MeV/c. Applying these corrections to the momentum of the slow pion in our data, we find a shift in the fit value of Q_0 , -4 keV for all the samples, and a negligible change in the width. We evaluate uncertainties in the energy scale by varying an overall momentum scale to change the $K_s \rightarrow \pi^+\pi^-$ mass by ± 30 keV, the uncertainty on that mass [8], and applying the statistical errors we obtain from the calculations of the momentum corrections discussed above.

Table III summarizes the systematic uncertainties on the width of the D^{*+} and Q_0 .

In summary, we have measured the width of the D^{*+} by studying the distribution of the energy release in $D^{*+} \rightarrow D^0\pi^+$ followed by $D^0 \rightarrow K^-\pi^+$ decay. With our estimate of the systematic uncertainties for each of the three samples being essentially the same, we chose to report the result for the sample with the smallest statistical uncertainty, the minimally selected sample, and obtain

$$\Gamma(D^{*+}) = 96 \pm 4 \pm 22 \text{ keV}, \quad (3)$$

where the first uncertainty is statistical and the second is systematic. This is the first measurement of the width of the D^{*+} , and it corresponds to a strong coupling [1]

$$g = 0.59 \pm 0.01 \pm 0.07. \quad (4)$$

This is consistent with theoretical predictions based on heavy quark effective theory and relativistic quark models, but higher than predictions based on QCD sum rules. We

TABLE III. Systematic uncertainties on the width of the D^{*+} and Q_0 .

Source	Uncertainties in keV					
	Nominal		Tracking		Kinematic	
	$\delta\Gamma(D^{*+})$	δQ_0	$\delta\Gamma(D^{*+})$	δQ_0	$\delta\Gamma(D^{*+})$	δQ_0
Dependence on kinematics	16	8	16	8	16	8
Mismodeling of σ_Q	11	<1	9	4	7	<1
Fit correlations	8	3	9	4	9	5
Vertex reconstruction	4	2	4	2	4	2
Background shape	4	<1	2	<1	2	<1
Offset correction	2	3	6	10	3	5
Data digitization	1	1	1	1	1	1
Energy scale	1	8	1	8	1	8
Quadratic sum	22	12	22	16	20	14

also measure the mean value for the energy release in $D^{*+} \rightarrow D^0 \pi^+$ decay,

$$Q_0 = 5842 \pm 2 \pm 12 \text{ keV}, \quad (5)$$

where the first error is statistical and the second is systematic. Combining this with the mass of the charged pion, 139.570 MeV with an uncertainty less than 1 keV [8], we calculate

$$m_{D^{*(2010)^+}} - m_{D^0} = 145.412 \pm 0.002 \pm 0.012 \text{ MeV}. \quad (6)$$

This agrees with the value from the Particle Data Group, 145.436 ± 0.016 MeV, from a global fit of all flavors of $D^* - D$ mass differences.

We thank D. Becirevic, I. I. Bigi, G. Burdman, A. Khodjamirian, P. Singer, and A. Le Yaouanc for valuable discussions. We gratefully acknowledge the effort of the CESR staff in providing us with excellent luminosity and running conditions. This work was supported by the National Science Foundation, the U.S. Department of Energy, the Research Corporation, the Natural Sciences and Engineering Research Council of Canada, and the Texas Advanced Research Program.

*Permanent address: Brookhaven National Laboratory, Upton, NY 11973.

- [1] V. M. Belyaev *et al.*, Phys. Rev. D **51**, 6177 (1995) contains a recent survey summarizing and referencing previous theoretical literature. P. Singer, Acta Phys. Pol. B **30**, 3849 (1999); J. L. Goity and W. Roberts, JLAB-THY-00-45 (hep-ph/0012314); K. O. E. Henriksson *et al.*, Nucl. Phys. **A686**, 355 (2001); M. Di Pierro and E. Eichten, hep-ph/0104208, appear since that survey.
- [2] M. Wise, Phys. Rev. D **45**, R2188 (1992); G. Burdman and J. F. Donoghue, Phys. Lett. B **280**, 287 (1992); T. Yan *et al.*, Phys. Rev. D **46**, 1148 (1992); **55**, 5851(E) (1992); D. Becirevic and A. Le Yaouanc, J. High Energy Phys. **9903**, 021 (1999) contains a recent review referencing previous theoretical literature.
- [3] S. Barlag *et al.*, Phys. Lett. B **278**, 480 (1992).
- [4] The analysis is described in full detail in CLEO Collaboration, A. Anastassov *et al.*, CLNS 01/1741, CLEO 01-13 (to be published).
- [5] CLEO Collaboration, Y. Kubota *et al.*, Nucl. Instrum. Methods Phys. Res., Sect. A **320**, 66 (1992); T. Hill, Nucl. Instrum. Methods Phys. Res., Sect. A **418**, 32 (1998).
- [6] CLEO Collaboration, R. Godang *et al.*, Phys. Rev. Lett. **84**, 5038 (2000).
- [7] R. Brun *et al.*, GEANT3 Users Guide, CERN DD/EE/84-1.
- [8] Particle Data Group, D. E. Groom *et al.*, Eur. Phys. J. C **15**, 1 (2000).